The effect of rapid thermal annealing to device performance of InGaAs/AlGaAs quantum well laser diodes

P L Gareso[a*], M Buda[b], H H Tan[b] & C Jagadish[b]

[a]Department of Physics, Faculty of Mathematics and Natural Sciences, Hasanuddin University, Makassar 90245, Indonesia

[b]Department of Electronic Materials Engineering, Research School of Physical Sciences and Engineering,
The Australian National University, Canberra, ACT 0200, Australia

The effect of rapid thermal annealing to device performance of InGaAs/AlGaAs quantum well laser diode has been investigated using photoluminescence (PL), double-crystal X-ray diffraction (DCXRD), photo-response (PR) and lasing characteristic. X-ray measurement results show that there is an incorporation of carbon atom in lattice site of higly doped p^{++} GaAs contact layer. The photocurrent spectra at room temperature reveal that the relative intensity of 1e-1hh transition of annealed samples is much higher than that of as-grown samples and the peak became narrow. Stark shifts are much higher for the samples after annealing in comparison to the as-grown samples and this has been attributed to a decrease of the confining potential due to thermal interdiffusion. Characteristic of laser diodes shows that there is no significant degradation of lasing parameters after annealing has been observed and it has been found that the threshold current of annealed laser diodes are approximately four times less than as-grown laser diodes and this has been attributed to the electrical activation of carbon.

Keywords: Inter diffusion, Photocurrent response, Stark shifts, Thermal annealing

1 Introduction

Thermal annealing is an essential semiconductor device processing technique and is particularly useful for intermixing where high temperature is required to initiate the interdiffusion process between barrier and quantum well region. On the other hand, the high temperature annealing required for interdiffusion could adversely affect the quality of the quantum wells and device performance. Despite this disadvantage, quantum well intermixing (QWI) has been widely used to modify the band gap energy. In addition to this, quantum well intermixing can be used to tailor new devices and has found applications in semiconductor lasers, waveguides, and optoelectronic integrated circuit[1]. There are several methods commonly used to initiate the well-barrier intermixing such as impurity induced disordering[2], impurity-free vacancy disordering[1,3] and ion implantation induced disordering[4]. All these methods rely on the diffusion of defects across the heterointerfaces to initiate interdiffusion process. Many studies have reported the effect of dopants on the intermixing[5,6] but the effect of dopant diffusion in actual optoelectronic devices has not received much attention.

In this study, the influence of rapid thermal annealing to device performance of InGaAs/AlGaAs laser diode doped with carbon is investigated. For this purpose, a thin p-clad laser structures was grown where the top layers and cladding layers were doped with carbon atoms. The use of carbon as p-type dopant is motivated by the low value of the diffusion coefficient in comparison to conventional dopants such as Mg, Zn and Be[7-9]. Also, carbon is well suited to the fabrication on integrated optoelectronic devices that require interdiffusion steps where high temperature annealing is performing to initiate the well barrier interdiffusion. Furthermore, carbon doping demonstrates high doping concentration[10,11] and high solid solubility[12]. These features make carbon suitable for electronic and optoelectronic devices such as heterojunction bipolar transistors (HBTs)[13] and laser diodes[14,15].

The thin p-clad InGaAs/AlGaAs QW laser structures used in this study is asymmetric structure design that most of the optical field distribution lies in the n-type layers, near the substrate and only small part of the distribution is found near top surface. In addition to this, since the thin p-cladding layer is about 0.3 μm compared with the standard thickness of about 1-1.5 μm. The penetration of the optical mode

*Corresponding author (E-mail: pgareso@gmail.com)

into the top surface is sufficient to achieve the required gratting coupling by shallow etching.

2 Experimental Details

Low pressure metal-organic vapour deposition (MOCVD) was used to grow the laser structure thin p-clad asymmetric structure grown on n^+ GaAs substrate. The details of these asymmetric InGaAs/AlGaAs laser structures have previously been reported[16,17]. The thin p-clad layer has a nominal thickness of 0.3 µm and a doping concentration of $\sim 1 \times 10^{18}$ cm^{-3}. The top p^{++} GaAs contact layer was highly doped ($> 10^{19}$ cm^{-3}). Both $Al_xGa_{1-x}As$ p-cladding and GaAs contact layers were doped with carbon. The active region consists of two $In_{0.20}Ga_{0.80}As$ undoped QWs which were separated by $Al_{0.20}Ga_{0.80}As$ barrier layers, while the bottom n-type cladding layers were doped with Si. The schematic of the laser structures are summarized in Table 1. The samples were annealed under Ar flow in a rapid thermal annealer in the temperature range of 875-925 °C for 60 s. During annealing, the samples were sandwiched between two GaAs substrates to minimize arsenic loss. Double-crystal X-ray diffraction (DCXRD) measurements were performed to determine the strain caused by the C atoms. Photoluminescence (PL) measurements were performed at 77 K and at room temperature. The PL set-up consisted of a frequency-doubled diode-pumped solid-state laser (λ= 532 nm) for excitation and an InGaAs photodetector at the output slit of 0.5 m monochromator.

Table 1 – Details of the asymmetric InGaAs/AlGaAs QW laser structures used in this work

Layer type	Al composition (x)	Thickness	Doping
p^{++} GaAs	0.00	0.10 µm	C:$>10^{19}$ cm^{-3}
p $Al_xGa_{1-x}As$	0.60	0.30 µm	C: $\sim 10^{18}$ cm^{-3}
Grading $Al_xGa_{1-x}As$	0.60 → 0.20	0.16 µm	Undoped
GaAs	0.00	1.8 nm	Undoped
$In_{0.20}Ga_{0.80}As$ QW		6 nm	Undoped
GaAs	0.00	1.8 nm	Undoped
$Al_xGa_{1-x}As$	0.20	6 nm	Undoped
GaAs	0.00	1.8 nm	Undoped
$In_{0.20}Ga_{0.80}As$ QW		6 nm	Undoped
GaAs	0.00	1.8 nm	Undoped
Grading $Al_xGa_{1-x}As$	0.20 → 0.60	0.16 µm	Undoped
$Al_xGa_{1-x}As$	0.60	0.10 µm	Si : 10^{17} cm^{-3}
Grading $Al_xGa_{1-x}As$	0.60 → 0.30	0.02 µm	Si : 10^{17} cm^{-3}
$Al_xGa_{1-x}As$	0.30	0.22 µm	Si : 10^{17} cm^{-3}
Grading $Al_xGa_{1-x}As$	0.30 → 0.45	0.01 µm	Si : 10^{17} cm^{-3}
$Al_xGa_{1-x}As$	0.45	0.70 µm	Si : 5×10^{17}cm^{-3}
$Al_xGa_{1-x}As$	0.45	2.00 µm	Si : 10^{18} cm^{-3}
n^+ GaAs substrate			

Standard device processing techniques were applied to fabricate the 4 µm wide stripe devices. The p-ohmic contact was obtained by evaporating Au on the top p^{++} GaAs contact layer. The contact was unannealed in order to prevent optical attenuation due to radiation scattering at the Au/p^{++}/GaAs interface. Photocurrent (PC) measurements were performed at room temperature. In the photocurrent experiment light from tungsten filament lamp is spectrally resolved through a monochromator before being focussed on the sample. The light produces an excess of free carrier in the sample. The effect of an external electric field on the photocurrent can also be measured by varying the applied bias .

3 Results and Discussion

3.1 X-ray diffraction

Double crystal X-ray diffraction (DCXRD) is a non-destructive technique widely used in the analysis of material structure and is particular useful in determining the layer thickness, composition, and strain of epitaxial structures. In addition to this, the X-ray diffraction method is in principle a very accurate and powerful tool when used to extract the lattice constant and its contraction/expansion relative to the substrate. It relies on modeling the data using both the layer thickness and its lattice constant. It can easily resolve a value of a lattice contraction $\Delta a/a$=10^{-5} if the layer is fully strained and if the layer is thick enough (thicker than about 0.3 µm). In this study, the XRD was used to gauge the strain profile introduced into epilayers as a result of the high carbon doping concentration in the layer.

Figure 1 depicts the X-ray rocking curve for C-InGaAs/InGaAs QWs before and after annealing at temperature of 900 °C and 925 °C as well as simulation results. As shown in this figure, the features appearing on the left hand side of the main GaAs peak are related to the AlGaAs layers. While an additional small peak on the right hand side are related to the tensile strain caused by the incorporation of the smaller C atoms in the highly doped p^{++} GaAs contact layer. Annealing the samples at 900 °C or 925 °C makes the tensile peak more pronounced when compared with the as-grown sample indicating that a tensile component emerges in the laser structures. It is well known that only carbon incorporated in an As lattice site C_{As} is electrically active. The substitution of the arsenic site causes contraction if the carrier concentration is larger than 10^{19} cm^{-3}, due to a smaller covalent radius of carbon
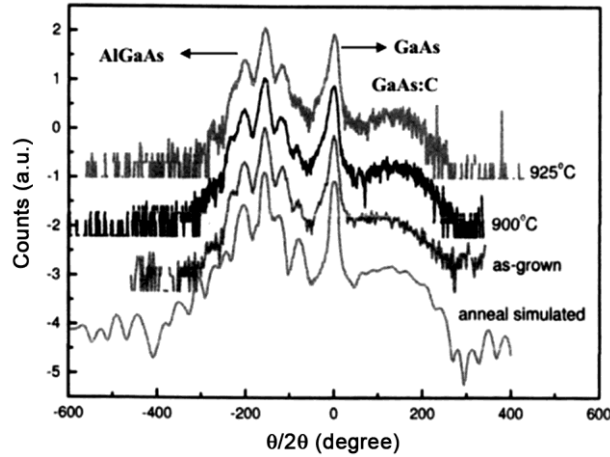
Fig. 1 — X-ray spectra of C-doped InGaAs/AlGaAs laser structures for as-grown and annealed samples at 900 °C and 925 °C for 60 s as well as simulation results
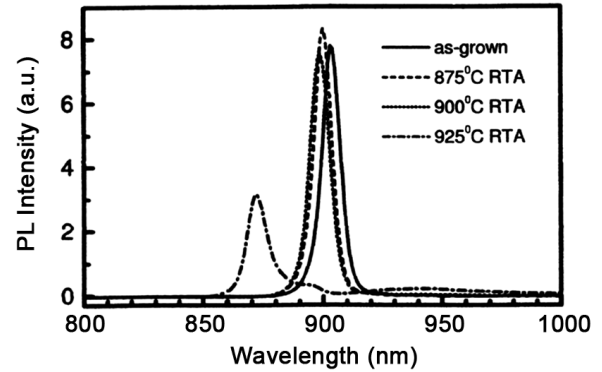

Fig. 2 — Low temperature (77 K) photoluminescence spectra of C-doped InGaAs/AlGaAs laser structures before and after annealing at 875 °C, 900 °C, and 925 °C for 60 s, respectively

(0.77 Å) compared[18,19] to As (1.20 Å) or Ga (1.26 Å). This lattice contraction can be easily monitored using DCXRD in InGaAs/AlGaAs/GaAs structures because all other layers are under compressive strain.

A simulation of the X-ray curve for annealed samples is also displayed in Fig. 1 which is consistent with the experimental results. For simulation results, we assume that the lattice site of GaAs incorporated with C atoms is a_{GaAs}: C = $(1-500\text{x}10^{-6}) \times a_{GaAs}$ and the thickness of GaAs layer is 0.10 μm. The simulation of the X-ray rocking curve indicates a layer of slight strain for the as-grown sample, with an average contraction of $\Delta a/a = 412 \times 10^{-6}$. For the annealed sample the lattice contraction is $\Delta a/a = 520 \times 10^{-6}$, corresponding to a 26 % increase in lattice contraction.

3.2 Thermal stability of InGaAs/AlGaAs

For interdiffusion application, the laser structures are required to be annealed at high temperature to initiate the interdiffusion between the quantum well and barrier region. However, the high annealing temperature required for intermixing could affect the physical properties of the samples which could have detrimental effects on laser diodes performance. Thereby, it is essential to study the thermal stability of the samples prior to fabricating the devices. For this purpose, the samples were annealed at various temperatures in the range of 875 °C – 925 °C to investigate the effect of thermal stability of the QW structures.

Figure 2 shows the low temperature PL spectra of InGaAs/AlGaAs QWs samples doped with carbon before and after annealing for 60 s at various temperatures ranging from 875 °C to 925 °C. The

emission peak at 903 nm originates from the quantum well region. A small blue shift was observed after annealing at 875 °C and 900 °C, while the PL intensities and PL linewidth were comparable to the as-grown samples. This indicates that only very little interdiffusion had occurred at these temperatures and the quality of the structures was preserved. At 925 °C, the PL intensity decreased and was accompanied by a relatively large wavelength shift and slight broadening of the linewidth. In addition to this, a smaller shoulder at 896 nm and a relatively broad peak at 942 nm were observed after annealing at 925 °C. These peaks are attributed to radiative transitions from point defects which are thermally generated during annealing. Therefore, based on this study of the dependence of thermal interdiffusion, annealing the sample at 900 °C for 60 s was chosen for subsequent experiment.

3.3 Photocurrent and lasing

In the case of photocurrent measurements, light from a tungsten filament lamp is spectrally resolved through a monochromator before being focused on the samples. The light produces an excess of free carriers in the sample. These free carriers move in response to local fields and an applied reverse bias, resulting in a photocurrent through an external circuit. The effect of an external electric field on the photocurrent can also be measured by varying the applied bias.

Figure 3(a) shows the photocurrent spectrum of as-grown laser diode at zero bias. As can be seen from this figure, two peaks are observed. One peak at 957 nm corresponds to the photogenerated carriers due to electron-heavy hole transition (1e-1hh). The other peak observed at 916 nm is attributed to the photogenerated carriers due to electron-light hole transition (1e-1lh). The
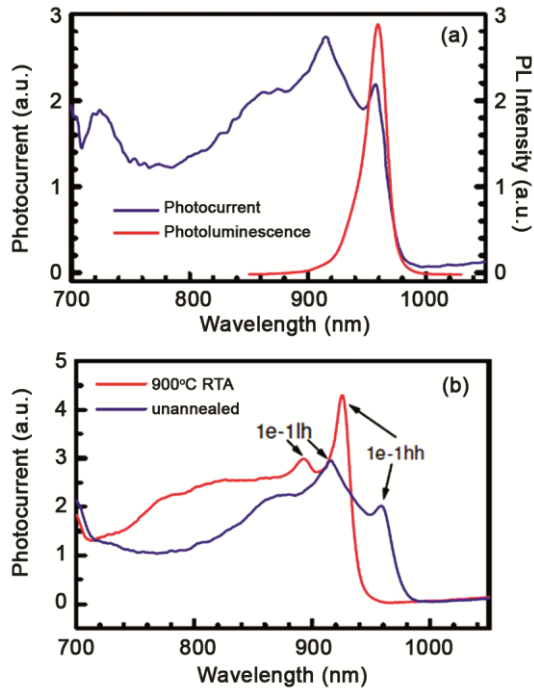
Fig. 3 — (a) Photocurrent spectrum of C-doped samples with 4 μm stripe and the diode length at approximately 1.5 mm. Room temperature photoluminescence spectrum of the as-grown samples is also shown for comparison and (b) photocurrent spectra of the C-doped as-grown sample and after annealing at 900 °C for 60 s

photoluminescence spectrum from as-grown sample is also shown for comparison. The photoluminescence peak is at 957 nm which is similar to the one obtained from the photocurrent spectra[20].

The room temperature photocurrent spectra of as-grown and annealed C-doped InGaAs/AlGaAs laser at zero bias are displayed in Fig. 3(b). After annealing, the quantum well peak emerges at 925 nm, blue shift by 33 nm from the as-grown sample. In addition, the relative intensity of the electron heavy-hole (1e-1hh) transitions of annealed samples is much higher than that of as-grown samples and the peak becomes narrower. This suggests the quality of the quantum well active region improves after annealing. In addition, the intermixing could also leads to an increase of the oscillator strength of the 1e-1hh transition and a shallower confining potential for electrons and holes.

Figure 4 displays the room temperature photocurrent spectra at various applied reverse bias of the samples before and after annealing. The probability of a photogenerated charge carrier escaping a quantum well and contributing to photocurrent increases with increasing applied bias. This was reflected in the observed photocurrent of the unannealed samples where the photocurrent became
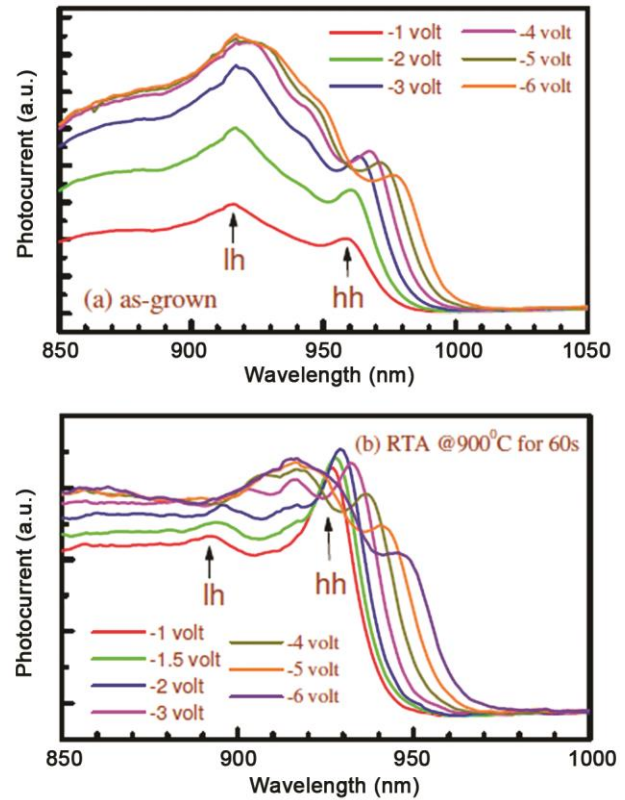

Fig. 4 — Photocurrent spectra of laser diodes at room temperature with various biases for the (a) as-grown and (b) after annealing at 900 °C for 60 s

saturated. Also, it is worth noting that the photogenerated carriers due to 1e-1lh transition were not much affected by the applied bias. In the case of annealed samples, the saturation of the photocurrent was seen when the bias at around –1.5 to –6 V. In this regime, the relative differences in the photocurrent intensities at different wavelength was obviously seen and these corresponded to a difference in absoption strength of different transitions. For both as-grown samples and annealed samples, the (1e-1hh) photocurrent peak progressively red shifted with increasing applied bias which was attributed to the quantum confined Stark effect.

The Stark shift of as-grown samples and annealed samples at 900 °C for 60 s as a function of applied bias in both heavy-hole and electron light hole transition are shown in Fig. 5. As can be seen from this figure, the Stark shift does not change significantly for 1e-1lh transition in the as-grown samples compared with the samples after annealing. In addition to this, the observed stark shift in 1e-1lh and 1e-1hh transitions are much greater for the annealed samples compared with the as-grown samples. These results indicate that the
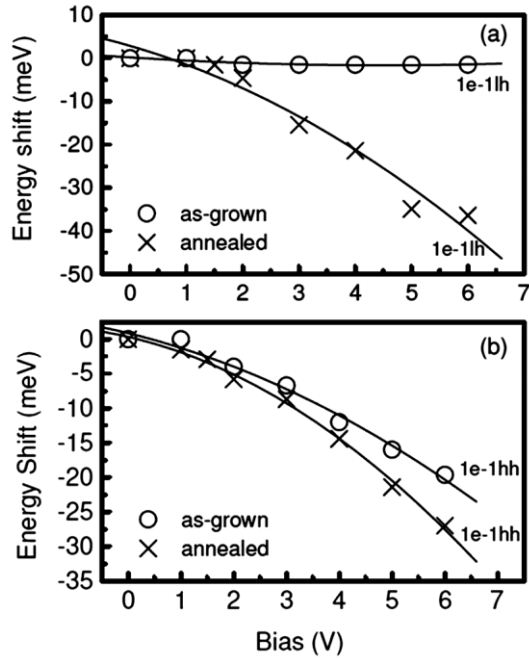
Fig. 5 — (a) 1e-1lh transitions and (b) 1e-hh transitions as a function of applied bias for as-grown samples and after annealing at 900 °C for 60 s. The solid lines are quadratic function fits
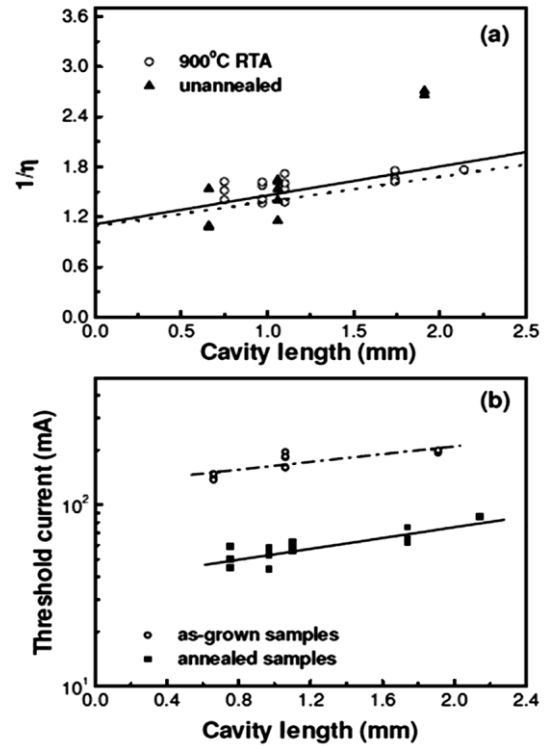

Fig. 6 — Characteristics of laser diodes showing (a) the inverse of the differential efficiency versus cavity length before and after annealing, and (b) the threshold current versus diode cavity length

confining potential due to the intermixing effects decreased after annealing.

The laser diodes were characterized by plotting the inverse external differential efficiency η and threshold current as a function of cavity length. The internal efficiencies η and the optical losses (the internal absorption coefficient) α are then drawn from the intercept and the slopes of the graph. Several factors might affect the internal absorption coefficient such as the contact and cladding layers, and the free carrier absorption in highly doped layers. In order to minimize free carrier absorption, the high doping was kept away from the active region and the region with large optical fields.

Figure 6(a) shows a plot of inverse external quantum efficiency against cavity length before and after annealing. The internal absorption coefficient α after annealing is around 2.6 cm^{-1} and 2.8 cm^{-1} before annealing with the internal efficiencies are around 99% for both set of diodes. These results show no significant degradation of lasing parameters after annealing at 900 °C for 60 s. Figure 6(b) illustrates a plot of the threshold current against cavity length. It is clearly observed that the threshold current decreased by approximately four times after annealing. The reduction in the lasing threshold current after annealing

is most likely due to reduction of grown defects and the activation of the carbon.

4 Conclusions

We have studied the effect of rapid thermal annealing to interdiffusion of InGaAs/AlGaAs laser diodes. X-ray measurement shows that there was an actication of carbon atoms in p^{++} GaAs contact layer. The photocurrent spectra of the as-grown samples and annealed samples were saturated at a certain bias where the peak positions were shifted to a longer wavelength. The observed red shift of 1e-1lh photocurrent peak was much greater for annealed samples compared with the as-grown samples. In addition to this, the stark shifts were much higher for the samples after annealing compared with the as-grown samples. These were attributed to a decrease of the confining potential due to intermixing effects of the annealed samples. Based on characteristics of laser diodes, there was no significant degradation of lasing parameters after annealing was observed and it was found that the threshold current decreased by around four times after annealing. The reduction in the lasing threshold current after annealing was due to

INDIAN J PURE & APPL PHYS, VOL. 55, MAY 2017

the activation of the carbon as well as reduction of grown-in defects.

Acknowledgement

References

1　Li E H, *Semiconductor quantum well intermixing*, (Gordon and Breach: Amsterdam), 2000.
2　Deppe D G & Holonyak N, *J Appl Phys*, 64 (1988) 93.
3　Fu L, Li Q, Kuffner P, Jolley G, Gareso P, Tan H H & Jagadish C, *Appl Phys Lett*, 93 (2008) 013504.
4　Tan H H, William J S, Jagadish C, Burke P T & Gal M, *Appl Phys Lett*, 68 (1996) 2401.
5　Guido L J, Cunningham B T, Nam D W, Hsieh K C, Plano W E, Major J S, Vesely E J, Sung A R, Holonyak N J & Stillman G E, *J Appl Phys*, 67 (1990) 2179.
6　Szafranek I, Szafranek M, Cunningham B T, Guido L J, Holonyak N J & Stillman G E, *J Appl Phys*, 68 (1990) 5615.
7　Kobayashi N, Makimoto T & Horikoshi Y, *Appl Phys Lett*, 50 (1987) 1435.
8　Kuech T F, Tischler M A, Wang P J, Scilia G, Potemski R & Cardono F, *Appl Phys Lett*, 53 (1988) 1317.
9　Cunningham B T, Guido L J, Baker J E, Major J S, Holonyak N J & Stillman G E , *Appl Phys Lett*, 55 (1987) 687.
10　Abernathy C R, Pearton S J, Caruso R, Ren F & Kovalchik J, *Appl Phys Lett*, 55 (1989) 1750.
11　Enquist P M, *Appl Phys Lett*, 57 (1990) 2348.
12　Kuech T F & Redwing J M, *J Cryst Growth*, 145 (1994) 382.
13　Abernathy C R, Ren F, Pearton S J, Fullowan T, Wisk P & Lothian J, *J Appl Phys*, 71 (1992) 1219.
14　Micovic M, Evaldsson P, Geva M, Taylor G W, Vang T & Malik R J, *Appl Phys Lett*, 64 (1994) 411.
15　Li H, Reinhardt H, Birth L & Bradford G, *J Cryst Growth*, 263 (2004) 181.
16　Buda M, Hay J, Tan H H, Wong-Leung J & Jagadish C, *IEEE J Quant Electron*, 39 (2003) 625.
17　Gareso P L, Buda M, Tan H H & Jagadish C, *Appl Phys Lett*, 85 (2004) 5583.
18　Li W & Pessa M, *Phys Rev B*, 57 (1998) 14627.
19　Giannini C, Fischer A, Lang C, Ploog K & Tapfer L, *Appl Phys Lett*, 61 (1992) 183.
20　Gareso P L, *Monolithic integration of different optoelectronic devices using IFVD method*, Proceedings of International Conference on Physics and Aplications (ICOPIA), Solo, Indonesia, 235 (October 2012).